

Accepted Manuscript

Phenol degradation by powdered metal ion modified titanium dioxide photocatalysts

Majeda Khraisheh, Lijun Wu, Ala' a H. Al-Muhtaseb, Ahmad B. Albadarin, Gavin M. Walker

PII: S1385-8947(12)01312-5
DOI: <http://dx.doi.org/10.1016/j.cej.2012.09.108>
Reference: CEJ 9869

To appear in: *Chemical Engineering Journal*

Received Date: 17 May 2012
Revised Date: 19 September 2012
Accepted Date: 21 September 2012

Please cite this article as: M. Khraisheh, L. Wu, A.H. Al-Muhtaseb, A.B. Albadarin, G.M. Walker, Phenol degradation by powdered metal ion modified titanium dioxide photocatalysts, *Chemical Engineering Journal* (2012), doi: <http://dx.doi.org/10.1016/j.cej.2012.09.108>

This is a PDF file of an unedited manuscript that has been accepted for publication. As a service to our customers we are providing this early version of the manuscript. The manuscript will undergo copyediting, typesetting, and review of the resulting proof before it is published in its final form. Please note that during the production process errors may be discovered which could affect the content, and all legal disclaimers that apply to the journal pertain.



1 **Phenol degradation by powdered metal ion modified titanium dioxide photocatalysts**

2
3
4 Majeda Khraisheh^a, Lijun Wu^b, Ala'a H. Al-Muhtaseb^c, Ahmad B. Albadarin^d, Gavin M.
5 Walker^{d,e}

6
7
8 ^a Department of Chemical Engineering, College of Engineering, Qatar University, P.O. Box
9 2713, Qatar

10
11 ^b Department of Civil, Environmental and Geomatic Engineering
12 University College London, UK

13
14
15 ^c Petroleum and Chemical Engineering Department, Faculty of Engineering, Sultan Qaboos
16 University, P.O. Box 33, Al-khod 123, Oman

17
18
19 ^d The Queen's University Environmental Science and Technology Research Centre, School of
20 Chemistry and Chemical Engineering, Queen's University Belfast, Northern Ireland, UK.

21
22 ^e Materials Surface Science Institute, Department of Chemical and Environmental Sciences,
23 University of Limerick, Ireland

24
25
26
27 * Corresponding author

28
29
30
31 Gavin M. Walker
32 E-mail: g.walker@qub.ac.uk

46 **Abstract**

47
48 Conventional water purification and disinfection generally involve potentially hazardous
49 substances, some of which known to be carcinogenic in nature. Titanium dioxide photocatalytic
50 processes provide an effective route to destroy hazardous organic contaminants. This present
51 work explores the possibility of the removal of organic pollutants (phenol) by the application of
52 TiO₂ based photocatalysts. The production of series of metal ions doped or undoped TiO₂ were
53 carried out via a sol gel method and a wet impregnation method. Undoped TiO₂ and Cu doped
54 TiO₂ showed considerable phenol degradation. The efficiency of photocatalytic reaction largely
55 depends on the photocatalysts and the methods of preparation the photocatalysts. The doping of
56 Fe, Mn, and humic acid at 1.0 M% via sol gel methods were detrimental for phenol degradation.
57 The inhibitory effect of initial phenol concentration on initial phenol degradation rate reveals that
58 photocatalytic decomposition of phenol follows pseudo zero order reaction kinetics. A
59 concentration of >1 g/L TiO₂ and Cu doped TiO₂ is required for the effective degradation of 50
60 mg/L of phenol at neutral pH. The rise in OH⁻ at a higher pH values provides more hydroxyl
61 radicals which are beneficial of phenol degradation. However, the competition among phenoxide
62 ion, Cl⁻ and OH⁻ for the limited number of reactive sites on TiO₂ will be a negative influence in
63 the generation of hydroxyl radical. The dependence of phenol degradation rate on the light
64 intensity was observed, which also implies that direct sunlight can be a substitute for the UV
65 lamps and that photocatalytic treatment of organic pollutants using this technique shows some
66 promise.

67
68 *Keyword:* Photocatalysts; Modified titanium dioxide; Photoreactor; Sol gel method; Wet
69 impregnation method; Phenol;

70 1- Introduction

71 While the world's population tripled in the 20th century, the use of renewable water resources
72 has grown six-fold. Poor access to good quality drinking water increases the risk of waterborne
73 diseases, which result in more than 10 million deaths. Diarrhoea alone is responsible for 2.2
74 million deaths each year, mostly among children under the age of five. This represents a
75 significant global problem, however a number of options available today for water disinfection
76 include chlorination, ozonation, iodine treatment, UV treatment, and boiling [1]. The ideal
77 solution would offer complete and full sterilization, without harming other forms of life; it
78 should also be inexpensive as well as non-corrosive [2].

79 The last 20 years has seen the development of two of the most interesting disinfection
80 alternatives: solar disinfection and TiO_2 photodisinfection under UV illumination [3]. The
81 combination of the two methods would result in a much greener, cheaper, more efficient, less
82 energy consuming technology, which could be produced and widely applied whilst causing no
83 harm to human health. Considering the fact that the areas of the world that lack access to safe
84 drinking water, which are also the world's poorest nations, have an abundance of sunlight
85 irradiation, the provision of this new technique can alleviate the current burden on the global
86 water supply and improve sanitation. However, the band-gap of TiO_2 is large, and is only active
87 in the ultraviolet region ($<400\text{nm}$), which is $< 10\%$ of the overall solar intensity, therefore the
88 light harvesting ability of TiO_2 is very limited [4]. The challenges in this area are the
89 development and mechanism investigation of an efficient TiO_2 based photocatalyst, which is
90 workable under sunlight [5]. Among many catalyst improvement techniques, doping has been
91 shown to be one of the most promising options, however its application in water disinfection
92 requires further investigation. Current photocatalysis is mainly focused on TiO_2 , and the basis for

93 its use is the employment of sunlight (or an artificial solar simulator lamp system) as an energy
94 input so that TiO₂ can be photoactivated by the UV spectrum of the irradiation [6].
95 The work of Matsunaga et al. [7] showed that TiO₂ was effective in photokilling *Lactobacillus*
96 *acidophilus* (gram-positive bacteria), *Saccharomyces cerevisiae* (yeast) and *Escherichia coli*
97 (gram-negative bacteria) under a metal halide lamp (12000 $\mu\text{e}\cdot\text{m}^{-2}\cdot\text{s}^{-1}$) for 1-2 h, moreover a
98 mechanism involved in the photooxidation of CoA was proposed. Ireland et al. [8] found that
99 the addition of electron acceptor-hydrogen peroxide at millimolar level had a positive impact on
100 the disinfection capability. Ide et al. [9] reported that the presence of deposited Au on the
101 supported layered TiO₂ could significantly improve its photocatalytic activity in the visible light
102 range. Zhang et al. [10] found that the absorption edge of N,S-codoped TiO₂ had a red-shift and
103 possessed the photocatalytic efficiency under visible light. Li et al. [11] proposed a visible
104 semiconductor sensitizer BiOI, which exhibits excellent photocatalytic activities on the
105 degradation of phenol under visible light irradiation. Photocatalytic tests showed that BiOI is an
106 effective sensitizer for improving the visible light photocatalytic activity of TiO₂. Zhu et al. [12]
107 investigated the photocatalytic disinfection of *E. coli* 8099 using Ag/BiOI composites under
108 visible light irradiation. The experimental results showed that the photocatalytic disinfection
109 efficiency of *E. coli* (5×10^7 cfu mL⁻¹) using 2.09%Ag/BiOI was almost 99.99% within 10 min
110 irradiation. Photocatalytic silver doped titanium dioxide nanoparticles (nAg/TiO₂) were
111 investigated for their capability of inactivating bacteriophage MS2 in aqueous media [13]. The
112 inactivation rate of MS2 was enhanced by more than 5 fold depending on the base TiO₂ material,
113 and the inactivation efficiency increased with increasing silver content. The increased production
114 of hydroxyl free radicals was found to be responsible for the enhanced viral inactivation.

115 Sontakke et al. [14] studied the photocatalytic inactivation of Escherichia coli with combustion
116 synthesized TiO₂ photocatalysts in the presence of visible light. It was found that photolysis
117 alone had a small effect on inactivation while the dark experiment resulted in no inactivation and
118 Ag/TiO₂ showed the maximum inactivation. At a catalyst loading of 0.25 g/L, all the combustion
119 synthesized catalysts showed better inactivation of E. coli compared to commercial Degussa P-
120 25 (DP-25) TiO₂ catalyst. An improved inactivation was observed with increasing lamp intensity
121 and addition of H₂O₂. A negative effect on inactivation was observed by addition of inorganic
122 ions such as HCO₃⁻, SO₄²⁻, Cl⁻, NO₃⁻, Na⁺, K⁺, and Ca²⁺. The photocatalytic inactivation of E.
123 coli remained unaltered at different pH of the solution.

124
125 However, problems such as the instability of the metal-doped titania and relatively low
126 absorption efficiency of the nonmetal-doped titania in the visible light region, are still
127 unresolved. Thus, exploring the highly-active photocatalysts with narrow band gap, which
128 function in the visible light region, has attracted remarkable attention. Accordingly, the aim of
129 this work was to explore the possibility of the removal of an organic pollutant (phenol) by the
130 application of TiO₂ based photocatalysts. The production of series of metal ions doped or
131 undoped TiO₂ was undertaken by a sol gel method and a wet impregnation method. A standard
132 photoreactor system was designed for such a purpose and the transport/kinetic processes of
133 phenol adsorption and removal were investigated.

134

135

136

137

138

139 2- Materials and Methods

140 2.1. Preparation of TiO₂ based photocatalysts

141 142 2.1.1 Sol-gel method

143 Materials used in this method are shown in Table (1). All the chemicals were laboratory grade. In
144 this method, Titanium (IV) isopropoxide was selected as metal alkoxide precursor because a
145 metal alkoxide with larger molecular weight is relatively stable, which is important in controlling
146 the reaction rate. Isopropanol, 2 (2-ethoxyethoxy) ethanol and ethanol were used as stabilizing
147 agents and solvents for the otherwise immiscible TTIP and H₂O. HCl and H₂SO₄ were used as
148 hydrolysis catalysts, while CuCl₂, CuSO₄ and Cu(NO₃)₂ were employed as dopants.

149 Undoped and Cu/TiO₂ catalysts were prepared via a sol gel method described by Ding and Liu
150 [15]. Titanium (IV) isopropoxide and alcohol (ethanol, 2(2-ethoxyethoxy) ethanol or
151 isopropanol) were vigorously stirred in a beaker. A mixture of fixed amount of deionised water
152 (DI water), acid (HCl or H₂SO₄) and alcohol was added drop-wise into the previous
153 TTIP/alcohol solution and magnetically stirred. After gelation, it was dried at 60°C in an oven
154 overnight. The powder was then annealed at a specific temperature for 2 h in furnace. Finally,
155 the catalysts was pulverized through 75µm sieves and kept in a sealed jar for use. For Cu doped
156 TiO₂, a given amount of copper precursor (1 ~ 10 mol % to TiO₂) was mixed with DI water, acid
157 and alcohol solution before the mixture was added into a TTIP/alcohol solution. The rest of the
158 preparation procedure was the same as with undoped TiO₂.

160 2.1.2 Wet-impregnation method

161 Materials used in this method are shown in Table (1). The preparation of Cu doped catalysts was
162 via a wet impregnation method described by Di paola et al. [16]. A given type/amount of Copper
163 dopant and TiO₂ P25 were added to 100 mL DI water. The mixture was then magnetically stirred

164 24 h followed by washing three times using DI water through filtration. Finally, solid was oven
165 dried at 60°C. Further calcination was carried out at 500°C for 2 h.

166 *2.2 Designation of prepared photocatalysts*

167
168 The denotation of the final catalysts was based on some of synthesis variables, including
169 preparation method, undoped or doped, difference in starting solution composition and annealing
170 temperature. The name of a catalyst can be seen in the format of ATBC. Here “A” stands for the
171 preparation method, it can be sol-gel method (SG) or Wet-impregnation method (IM). “T” is
172 short for TiO₂ and means it is a TiO₂ based photocatalyst. “B” stands for a dopant which could
173 be iron (Fe), Humic acid (HA), Manganese (Mn) but in most cases, it is copper (Cu). “C” stands
174 for different conditions in starting solution composition and annealing temperature, a detailed
175 lists corresponding to this nomenclature can be found in the list of synthesised materials. For
176 example, SGT9 represents a TiO₂ based photocatalyst, which was prepared by the sol-gel
177 method. In the standard sol gel procedure, the starting solution is composed of TTIP, Ethanol,
178 HCl and H₂O at a molar ratio of 1:8:0.06:1. There is no dopant addition in the dried catalysts and
179 the final annealing is at a temperature of 500°C for 2 h. Similarly, SGTCu43 is a TiO₂ based
180 photocatalyst which prepared from sol-gel method. In the standard sol-gel procedure, the starting
181 solution is composed of TTIP, isopropanol, H₂SO₄ and H₂O at a molar ratio of 1:80:0.06:14. It
182 was doped by copper at a level of 0.1 mol% towards TiO₂ and the final annealing conditions are
183 600°C for 2 h. The system with wet impregnated samples is simpler, they all share a same
184 starting TiO₂ P25 aqueous mixture and therefore, the number 2 in IMTCu2 stands for dopant
185 CuCl₂ is introduced at a level of 1.0 mol% before 500°C for 2 h.

186

187

188 *2.3 Measurement of photocatalytic activity*

189

190 *2.3.1 Solar box system*

191

192 The photoreactor consists of two chambers: the lamp and reactor chamber, with the lamp
193 chamber installed on top of the reactor chamber. Two UVA lamps are located in the lamp
194 chamber: (i) a commercial rupture fluorescent tube lamp and (ii) a fluorescent Blacklight Blue
195 tube lamp (18W, Silva) which transmit ultraviolet radiation peaking at 365 nm. In the reactor
196 chamber, Pyrex glass flasks are employed as batch reactors. Water samples taken from the solar
197 box system at specific time intervals were run at UV-Vis spectrophotometry for phenol
198 degradation experiment.

199

200 *2.3.2 Continuous flow system*

201 The schematic experimental set up for continuous flow system is shown in Figure (1). It
202 essentially consists of a photocatalytic reactor (PCR) with rectangle cooling jacket. Tap water is
203 circulated in the cooling jacket to control the temperature of PCR at 25°C (if not otherwise
204 stated). The PCR contains a UV lamp, 1 g/mL photocatalysts and magnetic stirrer. The aqueous
205 liquid running up the reactor was perpendicularly illuminated by immersed UV lamp whose
206 irradiation consistently strikes on the photocatalysts suspension. All parts of this reactor are
207 made from stainless steel in order to enhance the refracted light intensity. Photocatalysts are
208 located inside the inner circle container. Other main components of the system are the control
209 valve, the water grab sampler, a filter, connecting tubes and a water reservoir. The main function
210 of the water tank (WT) is to provide aeration of circulating bacterial suspension. The water grab
211 sampler is made up of water pump and flow meter, which provide the flow of the liquid in the
212 system. To sieve the photocatalyst, a filter has been incorporated downstream of the system. The
213 size of the PCR is around 700 cm³ and the total volume (V) of water suspension in the system is

214 controlled at 2000 cm^3 with the flow rate varied from 25 to $125 \text{ cm}^3 \text{ min}^{-1}$.

215

216 *2.4 Phenol photodegradation in water*

217

218 The evaluation of decontamination ability of the prepared catalysts was assessed by
219 photooxidation of phenol in water in the solar box system. To compare the degradation rates
220 between samples, it was ensured that the initial phenol concentration and irradiation intensity
221 were as close as possible. The evolution of the phenol concentration was monitored by UV–vis
222 spectrophotometry at its characteristic 270 nm band, using a centrifuged (4500 r.p.m for 5min)
223 aliquot ca. 2 mL of the suspension. All experiments were carried out in triplicates and DI water
224 was used throughout.

225 *2.5 Characterization and analytical tools*

226 *2.5.1 Point of zero charge determination*

227 In the experiment procedure described by Reymond and Kolenda: oxide suspensions with the
228 catalysts solid contents (weight percentage) as 0.01%,0.1%,1%,5%,10% were introduced in glass
229 beakers (capacity:10 mL). The beakers were filled with catalysts oxide suspensions in DI water
230 before sealed in order to minimize the residual air volume above suspension. The beakers were
231 then kept in air and shaken at 200 rpm at room temperature for 24 h. The pH was measured after
232 24 h of contact time, time for which pH equilibrium was reached in all the cases. It is considered
233 that the PZC value of the oxide is the pH value of the suspension having the higher solid content
234 when pH evolution with solid concentration is low.

235 2.5.2 Surface area measurement

236 The sample was pre-treated at 368 K for 1 h and 573K for 3 h under nitrogen, and then a
237 conventional 5-point BET nitrogen isotherm was taken at 77 K. All measurements were carried
238 out on a Micromeritics Gemini analyser. The amount of nitrogen admitted to the catalyst sample
239 was logged and the surface area calculations were carried out by the analyser.

240 2.5.3 UV-vis spectrophotometer

241 The concentration of phenol was measured on a double beam spectrophotometer (M350 double
242 beam, Camspec Scientific Instruments Ltd, Sawston, Cambridge, UK). To avoid the imperfection
243 of matching cuvettes when using a double beam, only one beam was used with a 1 cm quartz
244 cuvette. The zero was achieved with DI water and cuvette was regularly left to soak in
245 concentrated hydrochloric acid. The spectra of absorption of the phenol indicates the existence of
246 an absorption band corresponding to the transition $n \rightarrow n^*$ to a wavelength of 270 nm. The
247 indicated absorbance is proportional to the concentration in phenol, according to the law of Beer
248 Lambert in the studied concentration domain 0 - 100 mg/l.

249

250 3- Results and Discussion

251 3.1 Preliminary results

252 Preliminary tests were undertaken to check the viability of the solar box as a light input system.
253 A series of doped TiO_2 were prepared using the standard sol gel method as detailed in section
254 2.1.1 and a brief summary is provided in Table (2). The length of experiment was extended to 24
255 h in order to set a proper sampling time interval for later experiments. A typical trail time would
256 be set at around 10 h with 2 h sampling intervals. Blank samples were introduced using
257 irradiated phenol without the addition of photocatalysts.

258 As shown in Figure (2), the prepared dopant-free TiO₂ photocatalyst was very effective in the
259 reaction of phenol decomposition, and a linear dependence of phenol concentration versus time
260 was obtained. An analogous linear dependence was also observed for other doped TiO₂. From
261 these, consistent data were obtained using the Cu doped TiO₂, therefore, this was selected for
262 further investigations. On the other hand, humic acid doped TiO₂ and Mn doped TiO₂ (1 mol%
263 dopant: Ti⁴⁺) are almost photochemically inactive and low photoreactivity for phenol degradation
264 is observed for Fe³⁺ doped TiO₂.

265 The effect of individual metal ions on the photocatalytic activity of metal ion doped TiO₂ is a
266 complex area. An interpretation of reactivity order is difficult since it is probably the net result of
267 a combination of factors such as surface area, crystallinity, crystal size, band-gap energy etc.
268 Moreover, the addition of metals could be either beneficial or detrimental depending on whether
269 such metals decrease the rate of electron-hole recombination or act as electron-hole
270 recombination centers [17].

271 Using phenol as target organic pollutant and catalysts prepared from sol gel method, a significant
272 photoactivity decrease in metal ion doped TiO₂ compared with dopant free TiO₂ was also
273 reported in literature [18] with the dopant ions behaving as recombination centres of the
274 photoproduced charge carriers. The presence of dopant at a concentration level of 1 mol% seems
275 to be adequate to produce a negative influence by decreasing the density of surface-active
276 centers. However, it is still too early to conclude that doping is negative for the photodegradation
277 reactions. Dominant parameters such as character and concentration of the dopant, preparation
278 method and reaction regimes could be the key to tune up the reactivity of doped TiO₂.

279 *3.2 The effect of initial phenol concentration*

280 The photodegradation efficiency of phenol is related closely to its initial concentration. Higher
281 phenol concentrations lead to a decrease in the degree of degradation within the same time
282 period. The main reactions occur on the surface of the solid photocatalyst and at a high initial
283 concentration all catalytic sites are occupied. Further increase in the concentration can provide
284 excess reactant and also limits the adsorption of reaction intermediate on the reactive surface.
285 This prohibits the penetration of light reaching the surface and consequently less $\text{HO}\cdot$ is formed
286 resulting in a decrease of the observed zero-order rate constant.

287 The effect of the initial concentration of phenol is presented in Figures (3a) and (3b), and Table
288 (3). An increase in the initial phenol concentration substantially decreases in the degradation
289 rate. The remarkable inhibitory effect of the initial concentration of phenol on the apparent rate
290 constant has been reported with the photocatalytic decomposition of phenol following a negative
291 first order reaction kinetics [19,20]. However, there is no clear understanding of this negative
292 influence of initial phenol concentration. It has been proposed [21] that the phenoxide ions ArO^- ,
293 which are generated from the dissociation of phenol, maybe compete with and replace the
294 adsorbed OH^- on the limited number of reactive positions on the surface of catalysts. Then the
295 generation of $\text{OH}\cdot$ will be reduced since there are fewer active sites for the generation of $\text{OH}\cdot$
296 radicals. It is also worth noting that Phenol is always adsorbed on the TiO_2 surface in a
297 phenoxide ion [22].

298 At a concentration of 20 mg/L, there seems to be sufficient reactant molecules for the reactive
299 sites, however, a further increase in the concentration may prohibit the penetration of light.
300 Meanwhile, an excess phenol concentration increases the concentration of reaction intermediates to
301 be treated, which in turn also compete with the phenol for the reactive sites on the TiO_2 surface.

302 In the photomineralization of organic pollutants sensitized by TiO₂, it has been traditionally
 303 reported that the initial rate of disappearance of the pollutant fits a Langmuir–Hinshelwood (L–
 304 H) kinetic scheme [23]. The Langmuir-Hinshelwood (L-H) kinetic model assumes rapid,
 305 reversible adsorption of a reactant on the catalyst surface prior to reaction. The L-H rate equation
 306 is of the form:

$$307 \quad r_o = -\frac{d[C]}{dt} = \frac{k.K[C]}{1 + K[C]} \quad (1)$$

308 Where: r_o is the initial rate of disappearance of the organic substrate; k is a rate constant for the
 309 reaction ($\text{mmol L}^{-1} \text{min}^{-1}$), reflecting the limiting rate of reaction at maximum coverage under the
 310 given experimental conditions; K is the constant for adsorption of the organic substrate onto the
 311 TiO₂ surface (L mmol^{-1}); and C is the concentration of the organic substrate (mmol L^{-1}) in
 312 solution.
 313

314 The above equation can be inverted to solve for k and K .

$$315 \quad \frac{1}{r_o} = \frac{1}{K} + \frac{1}{k.K[C]} \quad (2)$$

316
 317 The slope and intercept from a plot of $1/r_o$ versus $1/[C]$ can be used to determine k and K .
 318
 319 Phenol oxidation data for both undoped and Cu doped TiO₂ at pH 5 were plotted using Equation
 320 (2) with reasonably good fits ($R^2 > 0.95$). The rate constant and the binding constant for TiO₂
 321 catalyst are $-0.16 \times 10^{-3} \text{ mmol L}^{-1} \text{ min}^{-1}$ and $-17.57 \text{ L mmol}^{-1}$, respectively, while for Cu/TiO₂
 322 they are $-0.5 \times 10^{-4} \text{ mmol L}^{-1} \text{ min}^{-1}$ and $-15.67 \text{ L mmol}^{-1}$, respectively. Traditionally, k is taken to
 323 represent the Langmuir absorption constant of the species (organic substrate) on the surface of
 324 TiO₂, and K is a proportionality constant which provides a measure of the intrinsic reactivity of
 325 the photoactivated surface with organic substrate [23]. The L-H rate constants at pH = 6.3

326 derived from Equation (2) for both catalysts showed the same order of reactivity, but the
327 undoped TiO_2 is almost 3 times more active than Cu doped TiO_2 . However, it is generally
328 assumed that both rate constants and orders are only “apparent”. They serve to describe the rate
329 of degradation, and may be used for reactor optimization, but they have no physical meaning,
330 and may not be used to identify surface processes.

331 *3.3 The effect of catalyst dose*

332 To increase the performance of heterogeneous photocatalytic process, one common way is to
333 increase the contact area of TiO_2 along the light path. The amount of catalyst used is also related
334 to cost effectiveness. A low mass of catalyst requires an extension of light exposure and
335 hydraulic retention time which increases the cost effectiveness. On the other hand, an excessive
336 amount of catalyst has cost implications and potential to reduce photoactivity due to increased
337 turbidity of the suspension. Hence, it is important to find the optimal amount catalyst mass for
338 the system.

339 To study the influence of catalyst mass, the quantity of catalyst was varied whilst keeping the
340 concentration of phenol solution equal to 50 mg/L. Figures (4a) and (4b) illustrated the influence
341 of catalyst mass on the degradation of phenol, in the range from 0.1 g/L to 2 g/L. It is illustrated
342 that phenol concentration decreases monotonically with an increase in catalyst mass in the water.
343 It is obvious that the higher catalyst mass, the higher the area of the reactive surface available for
344 adsorption and reaction will be. But the effect of catalysts dose cannot be indefinitely beneficial.
345 Above a certain level, the degradation rate will remain constant even with increased catalysts
346 loading. This rule is more obvious with TiO_2 in Table (4). As the concentration of the catalyst
347 increases, the amount of adsorbed photons as well as phenol molecules increases with respect to
348 the number of catalysts molecules. The concentration in the area of illumination also increases

349 and thus the reaction rate is enhanced. All studies of photocatalysis note the existence of an
 350 optimal concentration of TiO₂. It can be concluded that a suitable amount of TiO₂ for the
 351 photocatalytic reaction is approximately 1-3 g/L depending on types of reactor and TiO₂ powders
 352 [19, 21]. In our experiment, the catalyst loading is approximately 1.5 g/L for undoped TiO₂,
 353 while it can be in excess of 2 g/L for Cu doped TiO₂. Previous researchers suggest [24] that
 354 high-TiO₂ dose might lead to aggregation of the catalyst particles accompanied by reduction in
 355 reactive sites. Furthermore, shielding effects may occur due to high turbidity along with high
 356 concentration of catalyst which prevents light penetration. A consequent rate decrease is always
 357 a possibility if the dose is increased above a certain limit and hence the catalyst concentration
 358 must be monitored to ensure efficient photodegradation.

359 3.4 The effect of solution pH

360 Industrial effluents may be basic or acidic and therefore the effect of pH should be investigated.
 361 The pH value of phenol solution has a significant influence on the photocatalytic process for a
 362 variety of reasons, including the TiO₂ surface charge state, the flat-band potential, and the
 363 dissociation of phenol. These processes all are strongly pH dependent. The relative
 364 concentration of functional groups on the surface of hydrated TiO₂ (TiOH₂⁺, TiOH and TiO⁻)
 365 varies depending on the pH, due to surface hydroxyl groups gaining or losing a proton.



370 For Degussa P25 TiO₂, pKa₁ = 4.5 and pKa₂ = 8. The pH of the point of zero charge, pH_{pzc}, can
 371 be calculated from half of the sum of pKa₁ and pKa₂: pH_{pzc} = 6.25. The surface of TiO₂ shows a
 372 net positive charge as pH decrease below the pH_{pzc} and the negative charged surface dominates

373 as pH increases above pH_{pzc} . Phenol ($\text{p}K_{\text{a}}= 9.95$) exists as a molecular form in a neutral and
374 weakly basic solutions. High pH value favours the dissociation of phenol into phenoxide ion
375 $\text{C}_6\text{H}_5\text{O}^-$. As illustrated in Figure (5), a decrease in pH decreases the degradation rate. There is
376 less discrepancy between the neutral and basic environment, as compared to acidic conditions,
377 which may be explained by the surface chemistry of the system. At a low pH = 3.3 the molecule
378 of phenol is non-dissociated (neutral) and the surface of TiO_2 is either at a neutral state (TiOH)
379 [24] or positively charged as suggested by Al-Ekabi et al. [25]. These researchers studied the
380 photocatalytic oxidation of chlorinated phenol solutions and observed that the protonation of the
381 TiO_2 surface at low pH might be responsible for the inhibition of TiO_2 -mediated adsorption of
382 chlorinated hydrocarbon. In this study, as the pH is adjusted with HCl, the Cl^- anions are also
383 adsorbed at the surface of TiO_2 . There is competition between the adsorption of the anions and
384 phenol, hence the generation of $\text{OH}\cdot$ radicals is retarded. In the case of substances which are
385 weakly acidic, the photocatalytic degradation of phenol increases at lower pH because of an
386 increase in adsorption. At $\text{pH}= 6.3$, which is near its theoretical isoelectric point, the surface of
387 TiO_2 is negatively charged while the phenol adsorption is at its maximum and the quantity of Cl^-
388 ions is lower [24]. Meanwhile, when the pH increases, the active hydroxyl groups on the TiO_2
389 surface increase accordingly. Consequently, a faster generation of $\text{OH}\cdot$ radicals accelerates the
390 phenol oxidation [21]. It is also consistent with the work of O'Shea and Cardona [26], who found
391 that the initial reaction rates for phenol degradation steadily increases in the pH range from 3.0 to
392 9.0, however a lack of significant acceleration in the initial reaction rates was found at higher
393 pH. Similarly in our experiment, there is no significant difference in the initial reaction rate at a
394 pH of 10.3. This can be attributed to the fact that phenol is entirely dissociated into phenoxide
395 ion, which will compete for the reactive sites with the $-\text{OH}$ groups and reduce the $\text{OH}\cdot$ radicals.

396 Meanwhile, there is a phenomenon of repulsion between the negatively charged surface of TiO₂
397 and phenoxide ions, which explains the decrease in the rate of phenol oxidation. Although the
398 pH dependence phenomena have been observed by many authors, detailed explanations are still
399 not conclusive. Okamoto et al. [27] studied the photocatalytic oxidation of a 1 mM phenol
400 solution with TiO₂ and suggested that the optimum pH value was 3.5. Augugliaro et al. [19]
401 found that the kinetic rate increased as the pH value increased to about 3, and then it decreased
402 steadily until a pH value of about 12.5, beyond which the reaction rate constant again sharply
403 increased. Some other investigators have reported no effect of pH on the rate of phenol removal.

404 *3.5 The effect of light intensity*

405 Since the TiO₂ powder is suspended in a stirred solution, the light intensity will affect the degree
406 of light absorption by the TiO₂ surface [21]. Previous investigators have also studied the light-
407 intensity effect on the phenol degradation [27]. There are two ways of varying the light source
408 intensity in our solar box system. One is to change the distance of light and batch reactor.
409 Another is simply changing the light input sources, comparing UVA light with natural sunlight.

410

411 *3.5.1 Comparison between dark and irradiation*

412 In our batch reactor system, the catalyst used in this experiment is TiO₂ P25. Control is achieved
413 by exposing phenol in the solar box system, while another flask containing phenol and the same
414 amount of TiO₂ is kept in the dark during the same experiment period.

415 It is evident in Figure (6) that the presence of both catalyst and irradiation act favourably in the
416 photocatalytic process. In the absence of TiO₂ P25, phenol can hardly be degraded during a time
417 period over 20 h. Similar trends can be observed for the absence of irradiation, which also
418 suggests that TiO₂ powder cannot promote the oxidation of phenol [21] and that the adsorption

419 of phenol is negligible in the dark. The decline of phenol in the presence of TiO_2 along with
420 UVA irradiation may be attributed to the photooxidation process rather than adsorption.

421

422 *3.5.2 Comparison between the position of flask container*

423 In our batch reactor system, 100 mL quartz flasks are employed as the container which can be
424 placed either in position “A” that is just next to the lamp assuming the distance to be 0 cm or
425 position “B” that has a distance of 10 cm from the lamp. It is clear from Figure (7) that the nearer
426 the flask is to the lamp, the more efficient the photodegradation of phenol in the solar box. The
427 obvious explanation is that in the position “A”, the same size flask received more irradiation than
428 the flask in position “B”. Hence, it suggests that in the design of reactor system, effort can be
429 made to reduce the space between the reactor and the lamp.

430

431 *3.5.3 Comparison between artificial UVA and sunlight*

432 The threshold wavelength corresponds to the band gap energy for the semiconductor catalyst,
433 e.g., for the TiO_2 catalyst having band gap energy of 3.02 eV, the ideal wavelength is 400 nm.
434 Sunlight therefore is a valid source of irradiation for the excitation of the catalyst and has a
435 considerable economic advantage. A direct comparison between the results with solar box
436 system and sunlight from a clear sky is shown in Figure (8). The control shows no sign of phenol
437 degradation under sunlight. In the presence of TiO_2 , the concentration of phenol drops to around
438 10 mg/l in 5 hours, indicating 80% degradation. By comparing the sunlight and the solar box, it
439 can be seen that the former is almost 4 times more efficient than the latter. Similarly, it has been
440 reported [28] that the time required for 90% degradation of the phenol in sunlight in the presence
441 of 0.1% TiO_2 suspension was 55 min, approximately 1.7 times less than with the 100 W medium

442 pressure mercury lamp. The results confirmed the possibility of substitute UV irradiation with
443 direct sunlight. At the same time, data obtained in the solar box system can be extrapolated from
444 the laboratory set-up to a larger scale with reasonable confidence.

445 *3.6 The effect of catalysts preparation method*

446 The properties of catalysts are very much dependant on the preparation methods, therefore, two
447 different preparation methods for doped TiO₂ were used as specified in Table (5). As depicted in
448 Figure (9), IMTCu2 exhibits a better efficiency than SGTCu17 in phenol degradation, both of
449 which are prepared from CuCl₂ at a same concentration. The different in preparation methods
450 determine the dopant concentration distribution in the TiO₂ lattice structure, which may explain
451 the variation in photoactivity. In the wet impregnation method, the dopants may be confined to
452 the surface and/or to a few top layers of TiO₂ particles as dispersed species due to the moderate
453 calcination temperatures. The dopants in the sol gel methods are homogenously “dissolved” in
454 the TiO₂, although further calcinations may change their concentration distribution, the sol gel
455 method may produce a more homogenous doped catalyst, which is not always favoured.

456

457
458
459
460
461
462
463
464
465
466

467 **Conclusions:**

468 In the solar box system with two 18W UVA lamps, undoped TiO₂ and Cu doped TiO₂ showed
469 considerable phenol degradation. The efficiency of photocatalytic reaction largely depends on
470 the photocatalysts and the methods of preparation the photocatalysts. The doping of Fe, Mn, and
471 humic acid at 1.0 M% via sol gel methods were detrimental for phenol degradation. The
472 unremarkable inhibitory effect of initial phenol concentration on initial phenol degradation rate
473 reveals that photocatalytic decomposition of phenol follows pseudo zero order reaction kinetics.
474 A concentration of at least 1 g/L TiO₂ and Cu doped TiO₂ is required for the effective
475 degradation of 50 mg/L of phenol at neutral pH. It was found that pH plays a major role in the
476 phenomena of adsorption of phenol onto TiO₂. The increase in OH⁻ concentrations at a higher pH
477 values is beneficial of phenol degradation. However, the competition between phenoxide ion, Cl⁻
478 and OH⁻ for the limited number of reactive sites on TiO₂ will be a negative factor in the
479 generation of hydroxyl radical. TiO₂ is not active in the dark and the adsorption is negligible. The
480 dependence of phenol degradation rate on the light intensity was investigated, with the results
481 implying that direct sunlight can be a substitute for UV lamps, and that photocatalytic treatment
482 of organic pollutants may be an efficient technique.

483

484

485

486

487

488

489

490 **References:**

- 491 [1] L.M. Fry, J.R. Mihelcic, D.W. Watkins, Water and nonwater-related challenges of achieving
492 global sanitation coverage, *Environ. Sci. Technol.* 42 (2008) 4298–4304.
493
- 494 [2] E.H. Goslan, S.W. Krasner, M. Bower, S.A. Rocks, P. Holmes, L.S. Levy, S.A. Parsons, A
495 comparison of disinfection by-products found in chlorinated and chloraminated drinking waters
496 in Scotland, *Water Res.* 43 (2009) 4698–4706.
497
- 498 [3] S. Valencia, F. Cataño, L. Rios, G. Restrepo, J. Marín, A new kinetic model for
499 heterogeneous photocatalysis with titanium dioxide: Case of non-specific adsorption considering
500 back reaction. *App. Cata. B: Env.* 104 (2011) 300–304.
501
- 502 [4] H. Sun, S. Wang, H. Ang, M.O. Tadé, Q. Li. Halogen element modified titanium dioxide for
503 visible light photocatalysis. *Chem. Eng. J.* 162 (2010) 437–447.
504
- 505 [5] D. Ravelli, D. Dondib, M. Fagnonia, A. Albinia, Titanium dioxide photocatalysis: An
506 assessment of the environmental compatibility for the case of the functionalization of
507 heterocyclics. *App. Cata. B: Env.* 99 (2010) 442–447.
508
- 509 [6] G. Hyett, M.A. Greenb, I.P. Parkina, Ultra-violet light activated photocatalysis in thin films
510 of the titanium oxynitride, $Ti_{3-x}O_{4-x}N_x$. *J. Photochem. Photobiol. A: Chem.* 203 (2009) 199–203.
511
- 512 [7] T. Matsunaga, R. Tomoda, T. Nakajima, H. Wake, Photoelectrochemical sterilization of
513 microbial-cells by semiconductor powders. *Fems Micro. Lett.* 29 (1985) 211-214.
- 514 [8] J.C. Ireland, E. Klostermann, W. Rice, R.M. Clark, Inactivation of *Escherichia coli* by
515 titanium dioxide photocatalytic oxidation. *Appl. Environ. Microbiol.* 59 (1993) 1668-1670.
- 516 [9] Y. Ide, M. Matsuoka, M. Ogawa, Efficient visible-light-induced photocatalytic activity on
517 gold-nanoparticle-supported layered titanate. *J. Am. Chem. Soc.* 132 (2010) 16762–16764.
518
- 519 [10] G. Zhang, X. Ding, Y. Hu, B. Huang, X. Zhang, X. Qin, J. Zhou, J. Xie, Photocatalytic
520 degradation of 4BS dye by N,S-codoped TiO_2 pillared montmorillonite photocatalysts under
521 visible-light irradiation. *J. Phys. Chem. C.* 112 (2008) 17994–17997.
522
- 523 [11] Y. Li, J. Wang, B. Liu, L. Dang, H. Yao, Z. Li, BiOI-sensitized TiO_2 in phenol degradation:
524 A novel efficient semiconductor sensitizer. *Chem. Phy. Lett.* 508 (2011) 102–106.
525
- 526 [12] L. Zhu, C. He, Y. Huang, Z. Chen, D. Xia, M. Su, Y. Xiong, S. Li, D. Shu, Enhanced
527 photocatalytic disinfection of *E. coli* 8099 using Ag/BiOI composite under visible light
528 irradiation. *Sep. Purif. Tech.* 91 (2012) 59–66.
529
- 530 [13] M. Liga, E. Bryan, V. Colvin, Q. Li, Virus inactivation by silver doped titanium dioxide
531 nanoparticles for drinking water treatment. *Water Res.* 45 (2011) 535-544.
532

- 533 [14] S. Sontakke, C. Mohan, J. Modak, G. Madras, Visible light photocatalytic inactivation of
534 *Escherichia coli* with combustion synthesized TiO₂. *Chem. Eng. J.* 189–190 (2012) 101– 107.
535
- 536 [15] X.Z. Ding, X.H. Liu, Synthesis and microstructure control of nanocrystalline titania
537 powders via a sol-gel process. *Mat. Sci. Eng. A-Struct. Mat Prop Microst Proc.* 224 (1997) 210-
538 215.
- 539 [16] A. Di Paola, E. Garcia-Lopez, S. Ikeda, G. Marci, B. Ohtani, L. Palmisano, Photocatalytic
540 degradation of organic compounds in aqueous systems by transition metal doped polycrystalline
541 TiO₂. *Cata Today.* 75 (2002) 87-93.
- 542 [17] J.C. Colmenares, M.A. Aramendia, A. Marinas, J.M. Marinas, F.J. Urbano, Synthesis,
543 characterization and photocatalytic activity of different metal-doped titania systems. *App. Cata.*
544 *A-General.* 306 (2006) 120-127.
- 545 [18] V. Brezova, A. Blazkova, L. Karpinsky, J. Groskova, B. Havlinova, V. Jorik, M. Ceppan,
546 Phenol decomposition using Mn⁺/TiO₂ photocatalysts supported by the sol-gel technique on
547 glass fibres. *J. Photochem Photobio A-Chem.* 109 (1997) 177-183.
- 548 [19] V. Augugliaro, L. Palmisano, A. Sclafani, C. Minero, E. Pelizzetti, Photocatalytic
549 Degradation of Phenol in Aqueous Titanium-Dioxide Dispersions. *Toxicolog. Env. Chem.* 16
550 (1988) 89-109.
- 551 [20] K. Okamoto, Y. Yamamoto, H. Tanaka, M. Tanaka, A. Itaya, Heterogeneous Photocatalytic
552 Decomposition of Phenol over TiO₂ Powder. *Bull. Chem. Soc. Japan.* 58 (1985) 2015-2022.
- 553 [21] T.Y. Wei, C.C. Wan, Heterogeneous Photocatalytic Oxidation of Phenol with Titanium-
554 Dioxide Powders. *Ind. Eng. Chem. Res.* 30 (1991) 1293-1300.
- 555 [22] M. Primet, P. Pichat, M.V. Mathieu, Infrared Study of Surface of Titanium Dioxides .2.
556 Acidic and Basic Properties. *J. Phy. Chem.* 75 (1971) 1221-1225.
- 557 [23] S. Malato, P. Fernandez-Ibanez, M.I. Maldonado, J. Blanco, W. Gernjak, Decontamination
558 and disinfection of water by solar photocatalysis: Recent overview and trends. *Cata. Today.* 147
559 (2009) 1-59.
- 560 [24] S. Bekkouche, M. Bouhelassa, N.H. Salah, F.Z. Meghlaoui, Study of adsorption of phenol
561 on titanium oxide (TiO₂). *Desalin.* 166 (2004) 355-362.
- 562 [25] H. Alekabi, N. Serpone, E. Pelizzetti, C. Minero, M. A. Fox, R.B. Draper, Kinetic-Studies
563 in Heterogeneous Photocatalysis .2. Tio₂-Mediated Degradation of 4-Chlorophenol Alone and in
564 A 3-Component Mixture of 4-Chlorophenol, 2,4-Dichlorophenol, and 2,4,5-Trichlorophenol in
565 Air-Equilibrated Aqueous-Media. *Langm.* 5 (1989) 250-255.
- 566 [26] K.E. Oshea, C. Cardona, The Reactivity of Phenol in Irradiated Aqueous Suspensions of
567 TiO₂ - Mechanistic Changes As A Function of Solution pH. *J. Photochem. Photobiol. A-Chem.*
568 91 (1995) 67-72.

- 569 [27] K. Okamoto, Y. Yamamoto, H. Tanaka, A. Itaya, Kinetics of Heterogeneous Photocatalytic
570 Decomposition of Phenol Over Anatase TiO₂ Powder. Bull. Chem. Soc. Japan. 58 (1985) 2023-
571 2028.
- 572 [28] R.W. Matthews, S.R. Mcevoy, Photocatalytic Degradation of Phenol in the Presence of
573 Near-UV illuminated Titanium-Dioxide. J. Photochem. Photobiol. A-Chem. 64 (1992) 231-246.

ACCEPTED MANUSCRIPT

574

Name	Chemical Formula	Manufacturer	Description
Sol-gel method			
Titanium (IV) isopropoxide(TTIP)	Ti(OC ₄ H ₉) ₄	Acros Organic, UK	metal alkoxides precursor
Anhydrous isopropanol	(CH ₃) ₂ CHOH	Acros Organic, UK	alcohol solvent
Anhydrous 2(2-ethoxyethoxy) ethanol	CH ₃ CH ₂ OCH ₂ CH ₂ O-CH ₂ CH ₂ OH	Acros Organic, UK	alcohol solvent
Anhydrous ethanol	CH ₃ CH ₂ OH	BDH chemicals, UK	alcohol solvent
37% Hydrochloric Acid	HCl	Fisher Chemicals, UK	hydrolysis catalyst
Sulphuric acid	H ₂ SO ₄	BDH chemicals, UK	hydrolysis catalyst
Anhydrous copper (II) chloride	CuCl ₂	Acros Organic, UK	dopant
Anhydrous cupric sulphate	CuSO ₄	BDH chemicals, UK	dopant
Anhydrous copper (II) nitrate	Cu(NO ₃) ₂	Fisher Chemicals, UK	dopant
Anhydrous Manganese chloride	MnCl ₂	Fisher Chemicals, UK	dopant
Iron(II) chloride	FeCl ₃	Fisher Chemicals, UK	dopant
Humic acid	n/a	Acros Organic, UK	dopant
Wet-impregnation method			
Anhydrous copper (II) chloride	CuCl ₂	Acros Organic, UK	dopant
Anhydrous cupric sulphate	CuSO ₄	BDH chemicals, UK	dopant
Titania P25	TiO ₂	DegussaCo. Germany	80% anatase, 20% rutile; BET area: 50 m ² g ⁻¹

Table 1: Materials used in sol-gel method.

575
576
577
578
579
580

581
582
583
584
585
586
587
588
589
590

Table 2: Summary of photocatalysts used in preliminary experiment.

Material	Sample	Treatment
Cu doped TiO ₂ from sol gel method	SGTCu17	Hydrolysis and condensation of sol mixture (TTIP: Ethanol: HCl: H ₂ O: CuCl ₂ = 1:8:0.3:1: 0.01) at room temperature and followed by drying at 500 °C for 2 h
Mn Doped TiO ₂ from sol gel method	SGTMn1	Hydrolysis and condensation of sol mixture (TTIP: Ethanol: HCl: H ₂ O:MnCl ₂ =1:8:0.3: 1:0.01) at room temperature and followed by drying at 500 °C for 2 h
Iron doped TiO ₂ from sol gel method	SGTFe1	Hydrolysis and condensation of sol mixture (TTIP: Ethanol: HCl: H ₂ O:FeCl ₃ =1:8:0.3: 1:0.01) at room temperature and followed by drying at 500 °C for 2 h
Humic acid doped TiO ₂ from sol gel method	SGTHA1	Hydrolysis and condensation of sol mixture (TTIP: Ethanol: HCl: H ₂ O: humic acid=1:8:0.3:1:0.01) at room temperature and followed by drying at 120 °C for 2 h
Undoped TiO ₂ from sol gel method	SGT5	Hydrolysis and condensation of sol mixture (TTIP: Ethanol: HCl: H ₂ O=1:8:0.3:1) at room temperature and followed by drying at 500 °C for 2 h

591
592
593
594
595
596
597
598
599
600
601
602
603

604
605
606
607
608
609
610
611
612
613
614
615

Table 3: The initial phenol concentration effect on phenol disappearance rate on TiO₂ (Sample SGT5) and Cu doped TiO₂ (Sample SGTCu17) suspension from different initial concentration: 10 mg/L, 20 mg/L, 50 mg/L and 100 mg/L. Container size= 100 mL, Catalyst dose = 1g/L, pH = 6.3, Temp = 25°C.

phenol 1/[C ₀], (L mol ⁻¹)	TiO ₂ (1/r ₀) (L min mmol ⁻¹)	Cu- TiO ₂ (1/r ₀) (L min mmol ⁻¹)
940	-1.681 × 10 ⁴	-5.908 × 10 ³
1880	-1.573 × 10 ⁴	-5.048 × 10 ³
4700	-1.147 × 10 ⁴	-3.518 × 10 ³
9400	-6.123 × 10 ³	-2.874 × 10 ³

616
617
618
619
620
621
622
623
624
625
626
627
628
629
630
631
632
633
634
635
636
637
638
639
640

641
642
643
644
645
646
647
648
649
650
651
652

Table 4: Rate constants and binding constants from Langmuir-Hinshelwood plots for phenol disappearance on TiO₂ (Sample SGT5) and Cu doped TiO₂ (Sample SGTCu17) suspension from different initial concentration: 10 mg/L, 20 mg/L, 50 mg/L and 100 mg/L. Container size = 100 mL, Catalysts dose = 1g/L, pH = 6.3, Temp = 25°C.

Catalysts	Rate constant k (mmol L ⁻¹ min ⁻¹)	Binding constant K (L mmol ⁻¹)
TiO ₂	-0.16×10^{-3}	-17.57
Cu/TiO ₂	-0.50×10^{-4}	-15.67

653
654
655
656
657
658
659
660
661
662
663
664
665
666
667
668
669
670
671
672
673
674
675
676
677
678
679
680

681
682
683
684
685
686
687
688
689

Table 5: The catalyst dose effect on phenol disappearance rate on TiO₂ (Sample SGT5) and Cu doped TiO₂ (Sample SGTCu17) suspension in different catalysts dose: 0.1, 0.5, 1.0, 1.5 and 2.0 g/L. Container size = 100 mL, initial phenol concentration = 50 mg/L, pH = 6.3, Temp = 25°C.

Catalyst (g L ⁻¹)	TiO ₂ r ₀ (g h ⁻¹ L ⁻¹)	Cu doped TiO ₂ r ₀ (g h ⁻¹ L ⁻¹)
0.1	-0.00197	-4.94 × 10 ⁻⁵
0.5	-0.00248	-4.15 × 10 ⁻⁴
1.0	-0.00298	-8.95 × 10 ⁻⁴
1.5	-0.00334	-9.85 × 10 ⁻⁴
2.0	-0.00338	-11.8 × 10 ⁻⁴

690
691
692
693
694
695
696
697
698
699
700
701
702
703
704
705
706
707
708
709
710
711
712
713
714
715
716
717
718
719
720
721

722
723
724
725
726
727

Table 6: Photocatalysts used in studying the effect of catalyst's preparation method.

Material	Sample	Treatment
Cu doped TiO ₂ from sol-gel method	SGTCu17	Hydrolysis and condensation of sol mixture (TTIP: Ethanol: HCl: H ₂ O: CuCl ₂ = 1:8:0.3:1:0.01) at room temperature and followed by drying at 500 °C for 2 h
Cu doped TiO ₂ from wet-impregnation method	IMTCu2	Magnetic stirring of aqueous mixture of CuCl ₂ and TiO ₂ P25 (molar ratio: 0.01) at room temperature for 24 h and followed by filtration, oven drying at 60 °C overnight and 500 °C for 2 h

728
729
730
731

732 **Figure Captions:**

733

734 **Figure 1:** Schematic layout of continuous flow system.

735

736 **Figure 2:** Phenol disappearance on TiO₂ (Sample SGT8) and doped TiO₂ suspension. Container
737 size = 25mL, Catalysts dose = 1g/L, initial phenol concentration = 50 mg/L, pH = 6.3, Temp =
738 25°C.

739

740 **Figure 3:** Zero order plots of phenol disappearance on (a) TiO₂ (Sample SGT5) and (b) Cu
741 doped TiO₂ (Sample SGTCu17) suspension from different initial concentration: 10mg/L,
742 20mg/L, 50mg/L and 100mg/L. Container size = 100mL. Catalysts dose = 1g/L, pH = 6.3, T =
743 25°C.

744

745 **Figure 4:** Phenol disappearance on (a) TiO₂ (Sample SGT5) and (b) Cu doped TiO₂ (Sample
746 SGTCu17) suspension in different catalysts dose: 0.1, 0.5, 1.0, 1.5 and 2.0 g/L. Container size =
747 100 mL, initial phenol concentration = 50 mg/L, pH = 6.3, T = 25°C.

748

749 **Figure 5:** Phenol disappearance from TiO₂ (Sample SGT5) suspension at different pH: 3.3, 6.3
750 and 10.3. Catalysts dose = 1g/L, initial phenol concentration = 50 mg/L, container size = 100
751 mL, T = 25°C.

752

753 **Figure 6:** Phenol disappearance on TiO₂ (Sample p25) suspension in different irradiation
754 conditions: Dark and solar box system UVA irradiation. Container size = 100 mL, Catalysts dose
755 = 1g/L, initial phenol concentration = 40 mg/L, pH = 6.3, T = 25°C. Control is used with absence
756 of TiO₂ in solar box system.

757

758 **Figure 7:** Phenol disappearance on TiO₂ (Sample P25) suspension in at different distance from
759 lamp: A is 0 cm and B is 10 cm. Container size = 100 mL, Catalysts dose = 1g/L, initial phenol
760 concentration = 40 mg/L, pH = 6.3, T = 25°C.

761

762 **Figure 8:** Phenol disappearance on TiO₂ (Sample SGT5) suspension in different irradiation
763 conditions: Direct sunlight and solar box system UVA irradiation. Container size = 100 mL,
764 Catalysts dose = 1g/L, initial phenol concentration = 50 mg/L, pH = 6.3. Control is used with
765 absence of TiO₂ in direct sunlight.

766

767 **Figure 9:** Phenol disappearance on Cu doped TiO₂ using sample prepared from different method
768 sol gel (Sample SGTCu17) and wet-impreganation (Sample IMTCu2) in solar box system UVA.
769 Container size = 100 mL, Catalysts dose = 1g/L, initial phenol concentration = 50 mg/L, pH =
770 6.3. Control is used with absence of Cu-TiO₂ in the same solar box system.

771

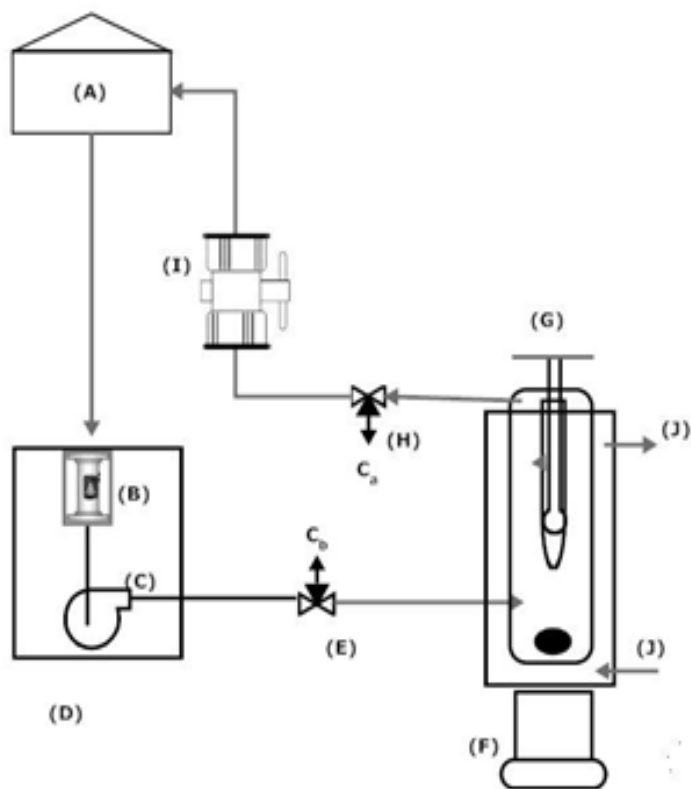
772

773

774

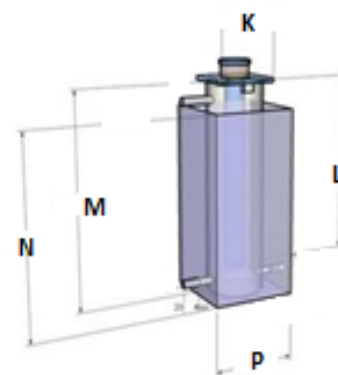
775

776 **Figure 1**
 777



LIST OF COMPONENTS

A - Tank
 B - Flow Meter
 C - DC Pump
 D - Water Grab Sampler
 E - Sampling Port C_a
 F - Magnetic Stirrer
 G - Lamp Reactor
 H - Sampling Port C_a
 I - Filter
 J - Cooling tap water

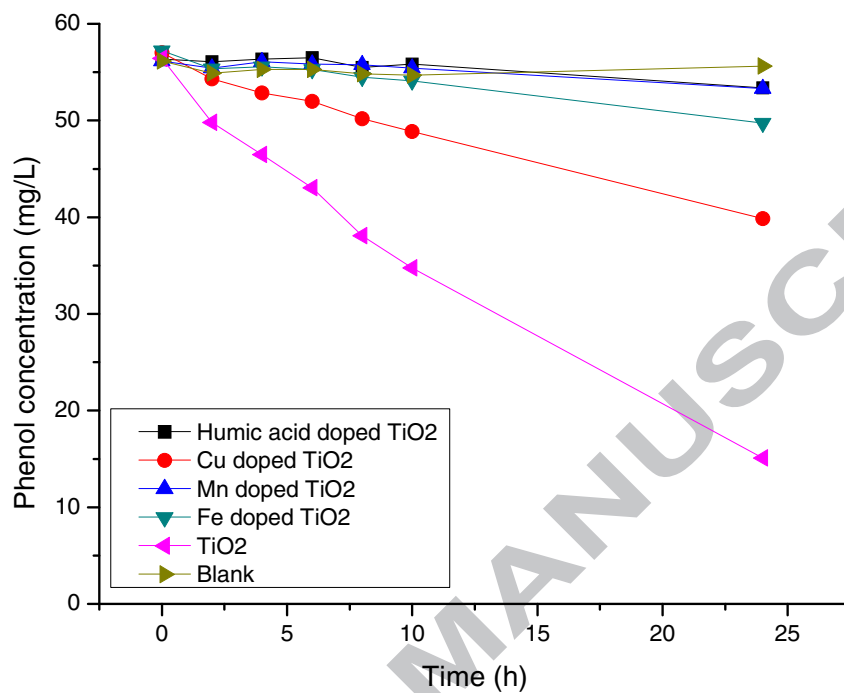


(G)

K= 71mm
 L= 220 mm
 M= 105mm
 N= 220mm
 P= 71mm

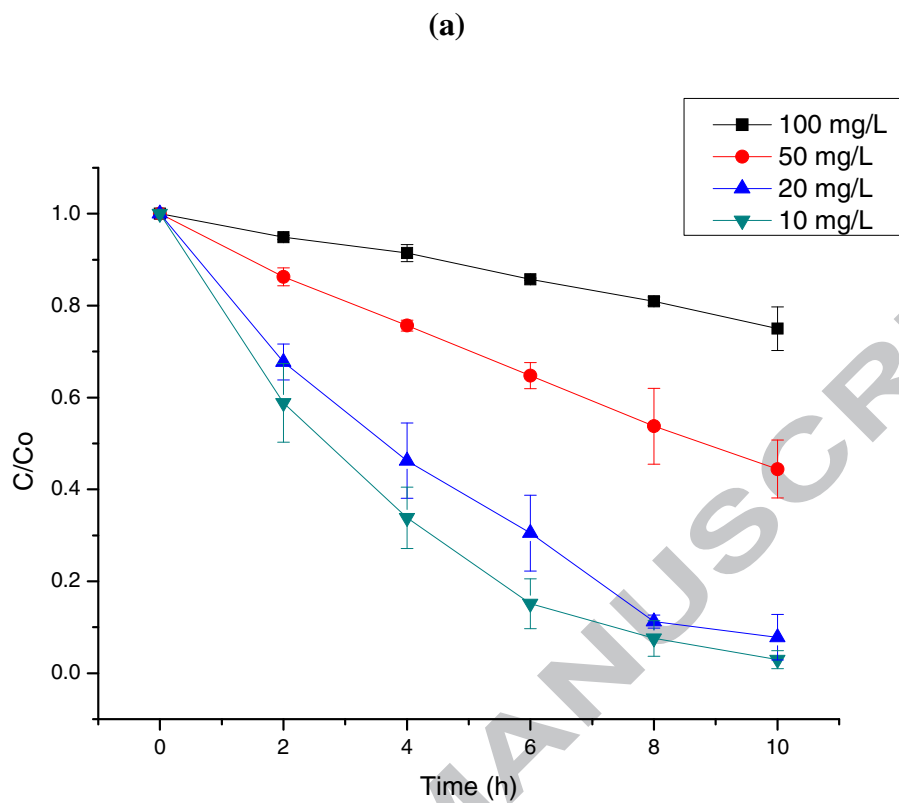
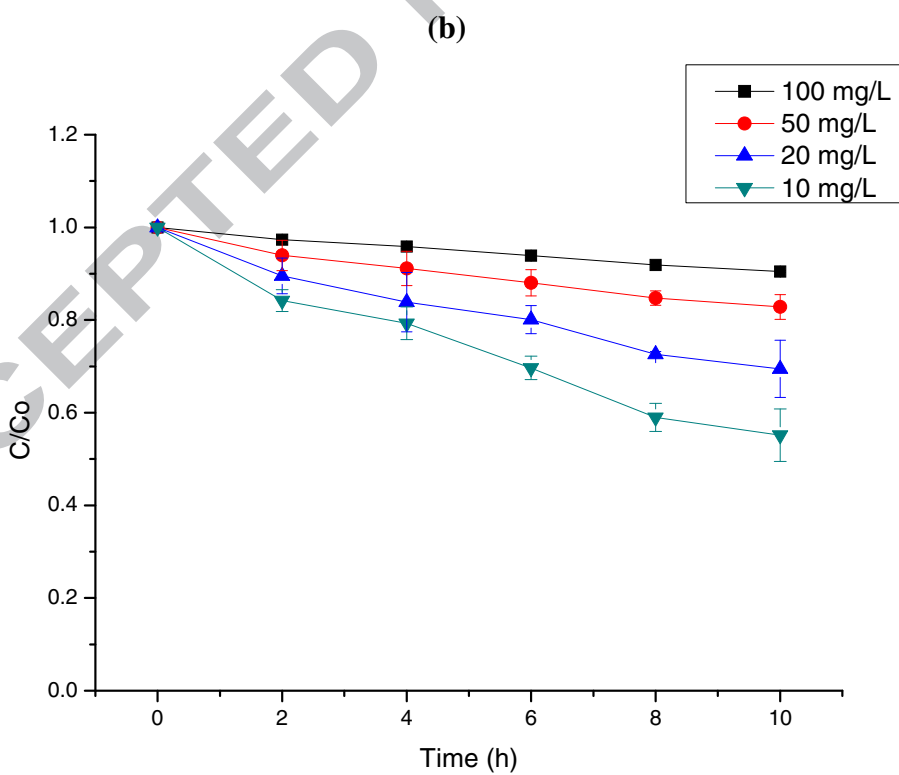
778
 779
 780
 781
 782
 783
 784
 785
 786
 787
 788
 789
 790
 791
 792
 793
 794
 795

796 **Figure 2**
797



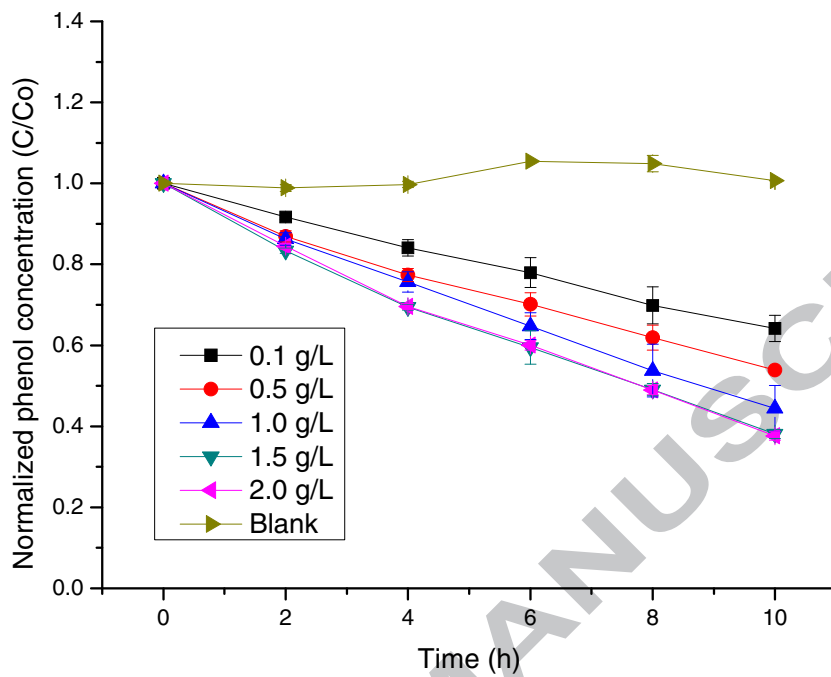
798
799
800
801
802
803
804
805
806
807
808
809
810
811
812
813

Figure 3

814
815816
817818
819 **Figure 4**

820

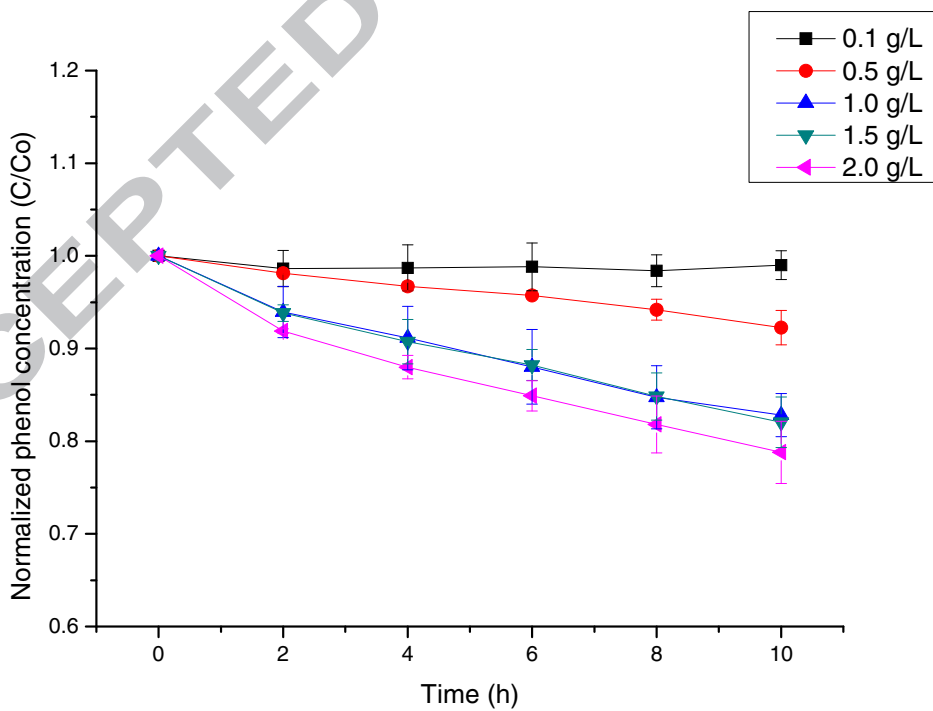
(a)



821

822

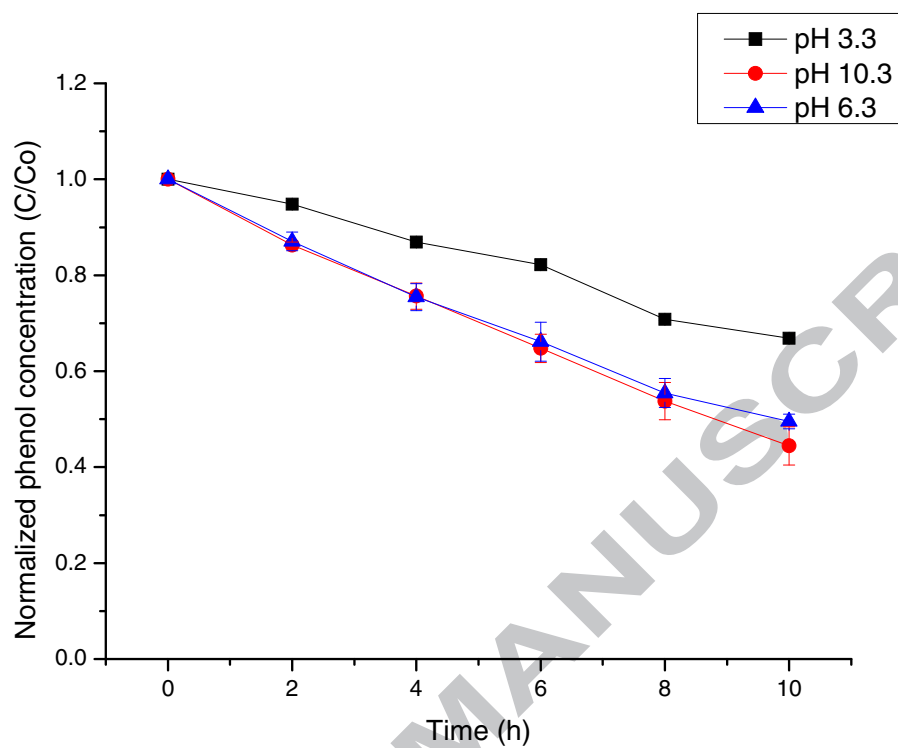
(b)



823

824 **Figure 5**

825



826

827

828

829

830

831

832

833

834

835

836

837

838

839

840

841

842

843

844

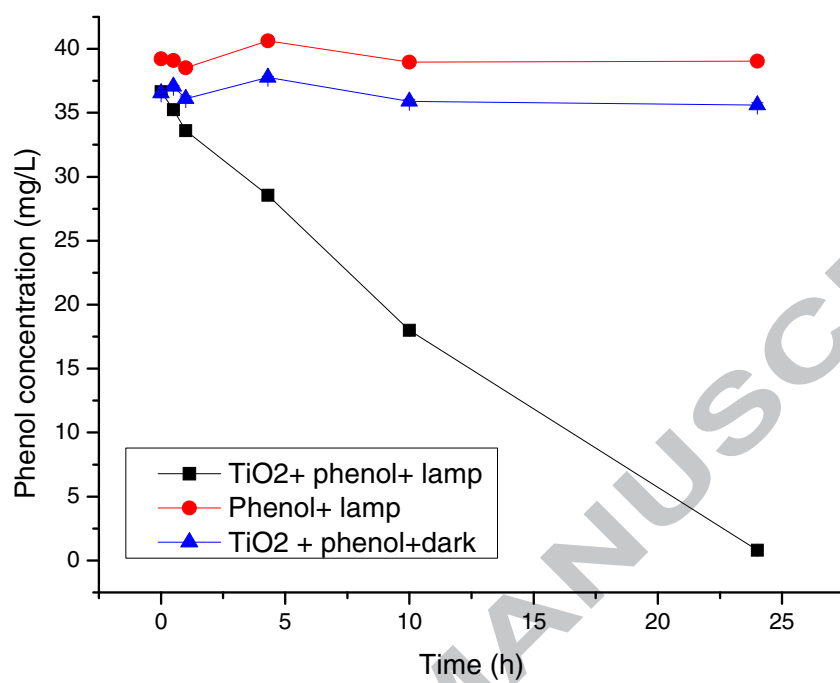
845

846

847

Figure 6

848



849

850

851

852

853

854

855

856

857

858

859

860

861

862

863

864

865

866

867

868

869

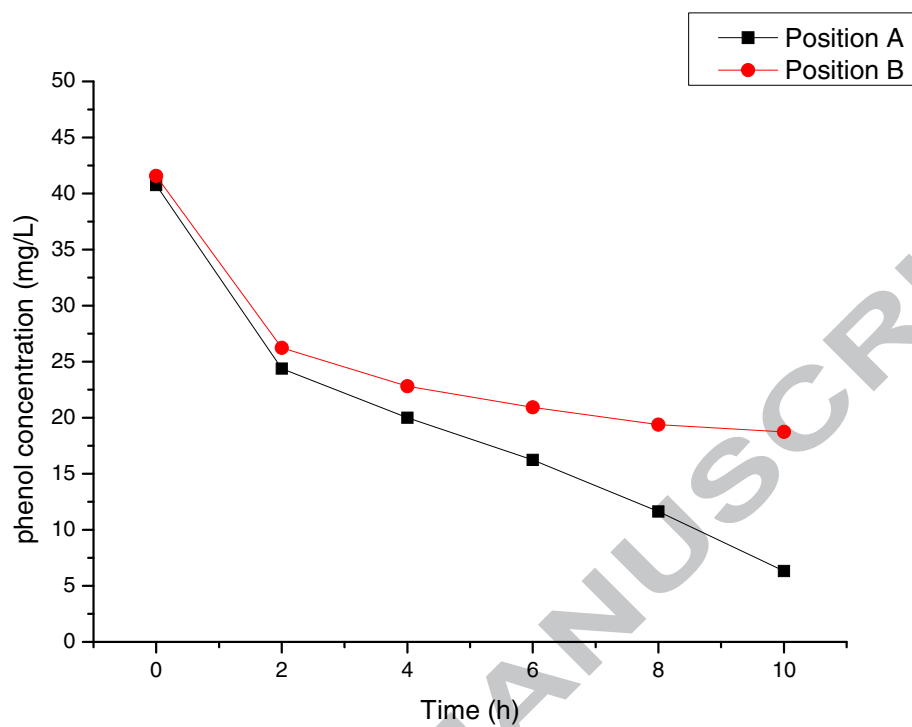
870

871

872

Figure 7

873



874

875

876

877

878

879

880

881

882

883

884

885

886

887

888

889

890

891

892

893

894

895

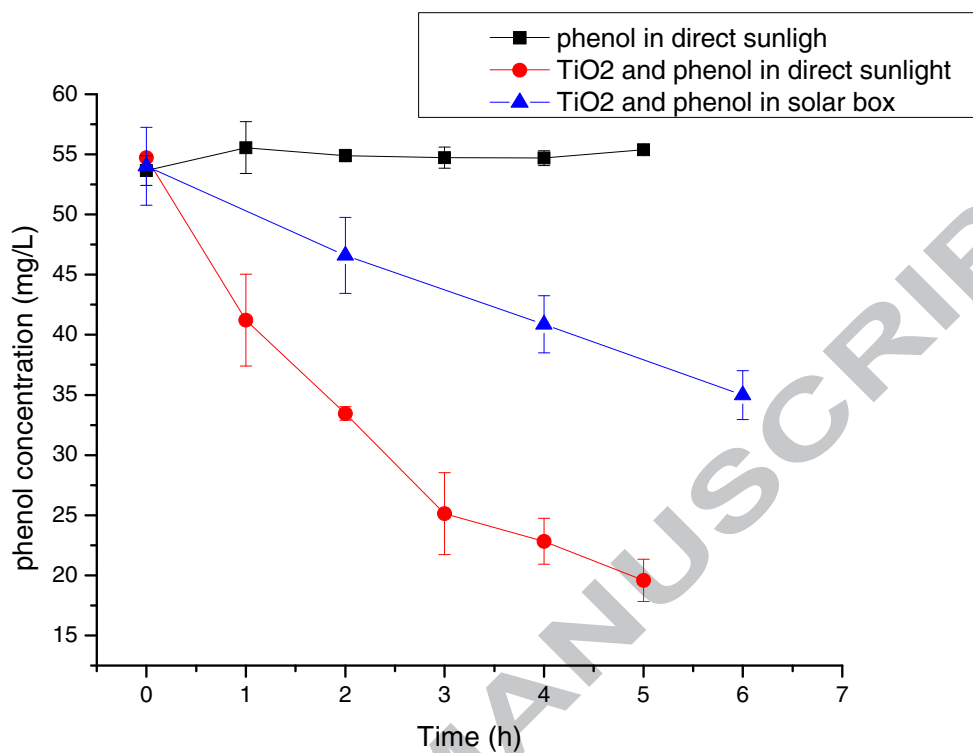
896

897

898

Figure 8

899



900

901

902

903

904

905

906

907

908

909

910

911

912

913

914

915

916

917

918

919

920

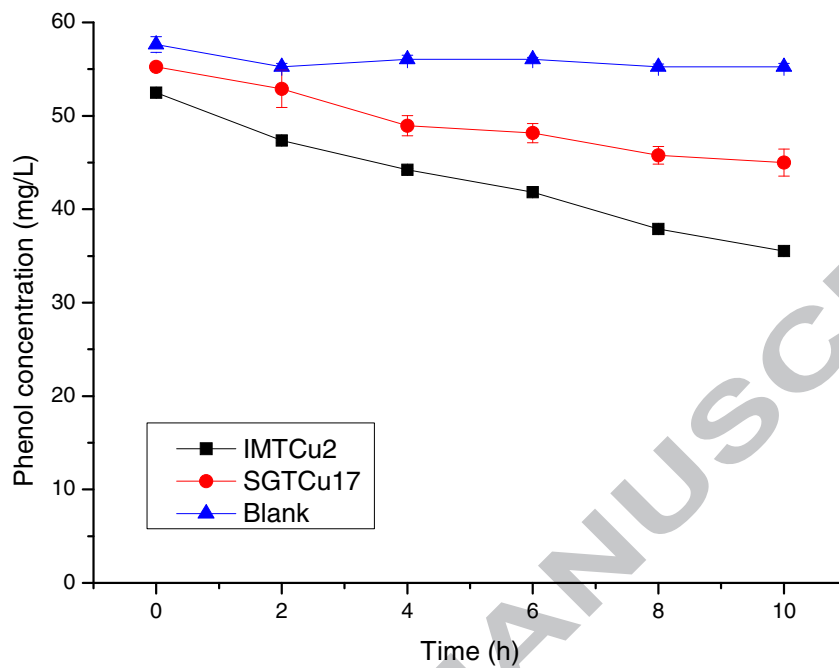
921

922

923

Figure 9

924



925

926

927

928

929

930

931

932

933

934

935

936

937

938

939 **Research Highlights:**

- 940 1- Removal of phenol by the application of TiO₂ based photocatalysts was explored.
- 941 2- Undoped TiO₂ and Cu doped TiO₂ showed considerable phenol degradation.
- 942 3- The efficiency of photocatalytic reaction depends on the methods of preparation.
- 943 4- Photocatalytic decomposition of phenol follows pseudo zero order reaction kinetics.
- 944 5- Direct sunlight can be a substitute for the UV lamps.

945

946

947

ACCEPTED MANUSCRIPT